Catena 213 (2022) 106156

Contents lists available at ScienceDirect

Catena

journal homepage: www.elsevier.com/locate/catena

Within-field spatial variations in subsoil bulk density related to crop yield and potential CO_2 and N_2O emissions

Peipei Yang [a], Arjan Reijneveld [b], Peter Lerink [c], Wei Qin [d], Oene Oenema [a,d,*]

[a] *Department of Soil Quality, Wageningen University, P.O. Box 47, 6700 AA Wageningen, the Netherlands*
[b] *Eurofins Agro, P.O. Box 170, 6700 AD Wageningen, the Netherlands*
[c] *IB-Lerink, Laan van Moerkerken 85, 3271 AJ Mijnsheerenland, the Netherlands*
[d] *China Agricultural University, Beijing 100193, China*

ARTICLE INFO

Keywords:
Subsoil compaction
Spatial variations
Semi-variogram analysis crop yield
Soil biological activity

ABSTRACT

Subsoil compaction is an increasing problem in modern agriculture, but is not easily recognized in practice, also because of possible within-field spatial variations. This paper addresses the question of how within-field spatial variations in soil bulk density and other soil characteristics relate to within-field spatial variations in crop yield and potential CO_2 and N_2O emissions from soil. Four fields (5 to 20 ha each) were selected at the suggestion of crop farmers, and sampled using a random soil sampling design (100 samples per field). Undisturbed soil samples were taken at depth of 5–10, 30–35, and 50–55 cm and soil bulk density and potential CO_2 and N_2O emissions measured under controlled conditions. At each sampling point, also top soil (0–20 cm) samples were taken for determination of pH, texture, SOM, and (micro)nutrients, and soil penetration resistance measurements and visual assessments of soil structure were made. Wheat yields were recorded with harvesters equipped with GPS and yield recorders.

Mean soil bulk density in the sub-soil (30–35 cm) ranged between fields from 1.36 ± 0.08 to 1.60 ± 0.11 g cm^{-3}. Mean wheat yields ranged between fields and years from 7.6 ± 0.6 and 11.3 ± 2.4 Mg ha^{-1}. Semi-variogram analyses showed that crop yields and soil properties were mostly spatially dependent; nugget-to-sill ratios were < 25% with ranges of 137 to 773 m. The ratio of CO_2 emissions to N_2O emissions was negatively related to soil bulk density, especially following N application.

In conclusion, within-field spatial variations in subsoil bulk density were successfully related to spatial variations in crop yield and potential CO_2 and N_2O emissions. The ratio of CO_2 emissions to N_2O emissions had a much greater response to spatial variations in soil bulk density than wheat yield. Our study suggests that N_2O emission factors may depend on (sub)soil bulk density.

1. Introduction

Subsoil compaction is an increasing problem in modern agriculture, but is not easily recognized in practice. Reports indicate that >68 million ha of agricultural land in the world have compacted subsoils. More than half of this area is in Europe (Wahlström et al., 2021; Hamza and Anderson, 2005). Soil compaction is commonly defined as the densification and distortion of soil by which total porosity and air-filled porosity are reduced and one or more soil functions are deteriorated (Schjonning et al., 2015; Huber et al., 2008; Banerjee et al., 2019). By reducing air permeability and limiting water infiltration, soil compaction may restrict root growth and nutrient uptake, which consequently affect soil functioning, including crop productivity, infiltration and storage of water and the decomposition of organic matter and transformation of nutrients (Keller et al., 2013). Compaction may be induced by natural factors, like alternate freezing-thawing and trampling of animals, as well as by human influences, i.e., through soil cultivation and heavy machinery (Keller et al., 2019).

Indicators for soil compaction include increases over time of soil bulk density, Relative Normalized Density (RND, defined as the actual dry bulk density divided by a critical or threshold bulk density), penetration resistance, and decreases over time of macro-porosity and infiltration capacity (Shah et al., 2017; Stolte et al., 2015; Chamen et al., 2015; van den Akker and Hoogland, 2011). Not all these indicators can be

* Corresponding author.
E-mail address: oene.oenema@wur.nl (O. Oenema).

https://doi.org/10.1016/j.catena.2022.106156
Received 7 September 2021; Received in revised form 14 February 2022; Accepted 19 February 2022
Available online 25 February 2022

measured easily in the field and they do not equally account for changes in the volume distribution of voids and their connectivity. As a result, relationships between indicators for subsoil compaction and soil functioning are not always straightforward (Keller et al., 2017; Horn et al., 1995).

Most of our understanding of subsoil compaction and its effects has been obtained in controlled condition experiments, also because there is no routine monitoring in farmers' fields of soil compaction and/or soil bulk density. Also, measurements of within field spatial variations in sub-soil bulk density have been carried out mostly in experimental fields (e.g., (Awal et al., 2019; Usowicz and Lipiec, 2017; Barik et al., 2014). Very few studies have examined spatial variations in subsoil bulk density in farmers' fields and have tried to relate these variations to spatial variations in crop yield and soil (microbiological) processes. The overall aim of our study was to increase the understanding of within-field spatial variations in (sub)soil bulk density in farmers' fields, and its relationships with spatial variations in crop yield and potential CO_2 and N_2O emissions (the latter as proxies for microbial activity). We hypothesized that (i) subsoil compaction is partly 'hidden' in spatial within-field variations in farmers' fields, and (ii) within-field spatial variations in subsoil compaction contribute to spatial variations in crop yield and soil microbial activity.

2. Materials and methods

2.1. Study area

The study was conducted in Hoeksche Waard, one of the islands (300 km^2) in the delta of southwest Netherlands (Fig. 1). It has a temperate maritime climate with cool summers and moderate winters. Annual mean precipitation is 850 mm, rather evenly distributed over the year. Hoeksche Waard is mainly used for arable farming (Ecorys, 2007); crop rotations include potato, sugar beet, winter wheat and horticultural crops (Crittenden et al., 2015; Steingrover et al., 2010). Most farms are family farms, but contractors may do part of the field work (e.g., manure application and potato, wheat and sugar beet harvesting). Farm size ranges between 50 and 500 ha, depending in part on crop rotations. Fields are flat (slope $<$ 0.1%) and are drained by surrounding ditches and subsurface drains at depth of 0.8 to 1.2 m with 10 to 30 m wide spacings. Many fields have become larger over time through closing ditches and re-parceling.

Soils have developed in marine deposits and have light clay to sandy clay texture in the upper half meter and loamy sand below. They are classified as Calcaric Fluvisols (WRB 2006). Mean groundwater level in winter is 45 $\sim$ 60 cm and in summer 140 $\sim$ 170 cm below soil surface.

2.2. Soil sampling design

Four fields with different shape and size (from 5.3 to 20.7 ha) and from four different farms were chosen (Fig. 1), following discussions with farmers of the foundation H-Wodka, which aims at enhancing the vitality of the rural agricultural community, nature and landscape in Hoeksche Waard through innovation. The farmers have concerns about the sustainability of current agricultural practices; they consider that spatial variations in soil compaction and soil fertility are possible barriers for increasing crop yield, but currently have no data and information to underpin these concerns. Farmers either had a 1:4 crop rotation (potatoes - winter wheat/vegetables/onions – sugar beet – winter wheat with cover crops) or a 1:3 crop rotation (potatoes – sugar beet/onions/vegetables – winter wheat). We selected fields in winter wheat; these fields had potatoes or sugar beet as pre-crops. Farmers ploughed the top 25 cm of soil with a moldboard plough, prior to seeding winter wheat in rows with a row distance of 12.5 cm. They aim at 250–300 wheat plants per m^2, 550 to 600 ears per m^2, and a grain yield of $\geq$ 10 Mg ha^{-1} yr^{-1}.

A total of 100 soil-sampling points were randomly selected within each field, using ArcGis software, in the spring of 2016. A total of 100 samples per field is generally considered to be an appropriate number for obtaining adequate insight in the spatial pattern of soil properties in agricultural fields of modest areas (Kerry and Oliver, 2007; Lawrence et al., 2020). At each sampling point, two sampling approaches were implemented. First, 5 samples of the topsoil (0–20 cm depth) were taken by augers within a circle with a radius of 5 m and then bulked and mixed (total weight about 2 kg) in plastic bags and transported within 5 h to a temperature conditioned room (4 °C) until further analysis. Secondly, undisturbed soil samples were taken at each point by stainless steel rings of exactly 100 cm^3, at three different depths. Soil sampling depths were based on observations in soil pits and discussions with farmers, and were uniform for all fields: 5–10 cm (plough layer), 30–35 cm (underneath the plough layer), and 50–55 cm, using the same auger hole. The undisturbed soil samples in stainless steel rings with plastic caps on the top and bottom were transported in wooden boxes within 5 h to a temperature conditioned room (4° C) and stored until further analysis. Each field was sampled within two to three consecutive days; all fields were

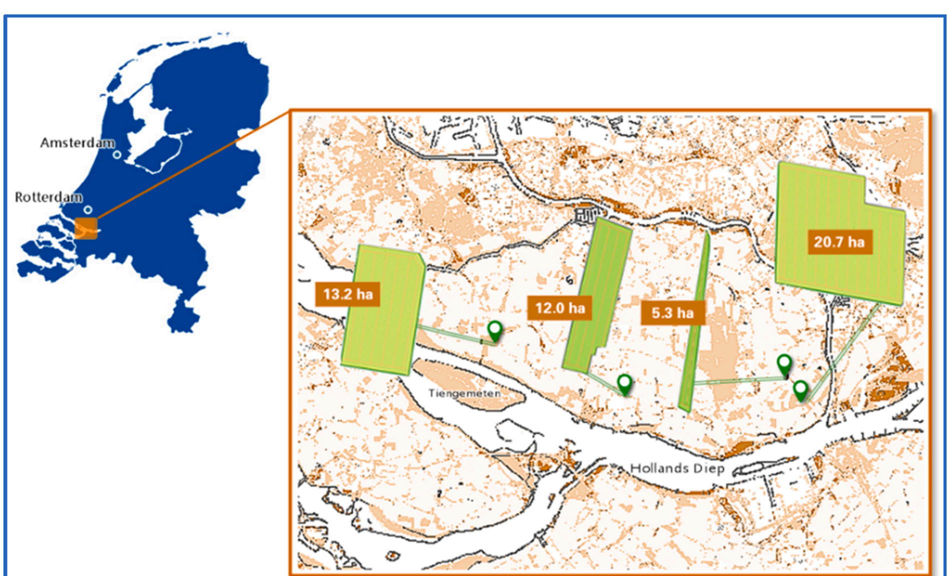

Fig. 1. Locations of the study area in the delta of south-west Netherlands. The inset shows the location of the four study fields.

sampled within a three-weeks period.

Penetration resistance was measured with a hand-held penetrograph (Stiboka penetrograph, Eijkelkamp Agrisearch Equipment, Giesbeek, the Netherlands). Within a circle with a radius of 5 m around each sampling point, the penetrometer was pushed into the soil manually at a fixed speed of about 30 mm s^{-1} (ASABE, 2006) at three randomly selected places. The area of the conical point was 1 cm^2 and the measuring depth was 0 to 80 cm. Results for depth of 5–10 cm, 30–35 cm, and 50–55 cm depth were averaged per sampling point. Penetrometer measurements of a single field were carried out within one day.

Soil structure assessments of the top soil (0–5 cm) were made on the basis of visual observations (Pulido Moncada et al., 2014; Mueller et al., 2009). Soil aggregation (structureless, weak structure, moderate structure, and strong structure), aggregate shape (granular, blocky, prismatic & columnar, and platy), and aggregate size (fine (<0.5 mm), medium (0.5–2 mm), coarse (2.0–5 mm), and very coarse (>5 mm)), were recorded at each sampling point.

2.3. Soil analyses

Samples from the topsoil (disturbed) were dried at 40 °C overnight. Near Infra-Red Spectroscopy was used for analyzing soil texture, soil organic matter, N-total, S-total and $CaCO_3$ according NEN-EN-ISO 17184 (ISO17184, 2014). The NIRS method was calibrated and validated on the basis of thousands of different soil samples from different areas in Europe (Reijneveld et al., 2022). The $CaCl_2$ extraction method (0.01 M; 1:10 (w/v) combined with Inductivity Coupled Plasma (ICP), Inductivity Coupled Plasma-Massa Spectrometry (ICP-MS) and segmented flow analyses (for NH_{4+} and NO_3^-) were used to measure plant-available (micro) nutrients (N, S, P, K, Mg, Na, Si, Fe, Zn, Mn, Cu, Co, B, Mo, Se), following NEN 5704 (NEN5704, 1996) and Van Erp (van Erp et al., 1998). The pH of the $CaCl_2$ extract was measured with a combination electrode and a potentiometer. These analyses were conducted by Eurofins Agro (https://www.eurofins.com/agro).

Undisturbed soil samples in stainless steel rings were measured for soil bulk density and potential emissions of N_2O and CO_2 in temperature (16 °C) and humidity (60%) conditioned rooms at Wageningen University. These emission determinations are meant to reflect the intrinsic characteristics of the soil samples at uniform environmental conditions (and not the actual or in-situ emissions in the field), and are therefore termed 'potential emissions'. Following pre-incubation at 16 °C for 1 day, the uncapped soil samples in stainless steel rings were put in 1 L PVC jars with screw lid with rubber septa for 60 min. Changes in potential N_2O and CO_2 concentrations in the headspace of the jars were measured via the photo-acoustic infrared gas analyser Innova 1312 (LumaSense Technologies A/S, Ballerup, Denmark). After these flux measurements, 12 ml $NaNO_3$ solution (2.4 g N L^{-1}) was gently sprayed on top of each soil sample, to simulate a common N fertilization of 150 kg per ha. One day (24 h), four and six days after fertilization, soil samples were put in jars again, and changes in N_2O and CO_2 concentrations in the headspace were measured; these are reported as 'induced N_2O and CO_2 emissions'.

N_2O emissions were calculated using the following equation:

$$F_{N_2O} = \frac{(C-O)}{VAT}\frac{28}{22.4} \tag{1}$$

Here, F is the emission rate (mg N_2O-N m^{-2} day^{-1}); C is the measured N_2O concentration (mg N_2O-N m^{-3}); O is the initial N_2O concentration (mg N_2O-N m^{-3}); V is the volume of the headspace (jar volume minus soil cylinder volume, L); A is the cross-sectional area of soil sample (m^2); T is the closing time (h); 22.4 is the number of moles per volume of air (1 L = 1/22.4 mol); 28 is the mol weight of N in N_2O (1 mol N_2O-N = 28 g N).

Similarly, CO_2 emissions were calculated using the following equation:

$$F_{C_2O} = \frac{(C-O)}{VAT}\frac{12}{22.4} \tag{2}$$

The parameters are the same as in equation (1), with 12 the mol weight of C (1 mol CO_2 = 12 g C).

After the potential CO_2 and (induced) N_2O emission measurements, soil samples in the rings were saturated with water, weighted, dried for 24 h at 105 °C and then again weighted to determine total pore volume and dry bulk density. The relative normalized density (RND) was estimated as the ratio of measured bulk density and a threshold value of bulk density (van den Akker and Hoogland, 2011). For sand and loamy soils (clay content < 16.7%), this threshold value is 1.6 g cm^{-3}; for soils with clay content > 16.7%, the threshold value is (1.75–0.009*clay content).

2.4. Yield recordings and calculation

Crop yields were recorded automatically during the harvesting of the wheat. The width of the harvesters was 5 m and the distance between yield recordings on-the-go were about 2 m. Recorded crop yields within circles around sampling points were averaged and then allocated to these soil sampling points. We used circles with a radius of 5 m and 10 m, to assess the uncertainty in allocation (Fig. 2). This allocation allowed us to relate spatial variations in crop yields to spatial variations in soil characteristics.

2.5. Data analysis

Spatial distributions of crop yield and soil properties were displayed by ArcGis 10.2.1, using Inverse Distance Weighted (IDW) interpolation (Lloyd 2005).

Spatial dependence and spatial distribution coefficients of crop yield and soil properties were displayed by GS + software, using the semi-variogram method (Gamma Design Software, GS + 9, 2008). The semi-variogram is the basic geostatistical tool for measuring spatial autocorrelation of a regionalized variable (Hohn, 1998). This method describes the structure and randomness of spatial variables, and quantitatively describes the spatial distributions.

First, all data per field were tested for normal distribution; data of most variables were not obedient to normal distributions (analyzed by the shapiro.test function of R studio (Kassambara, 2019). The data of these variables were then log-natural transformed. Exponential, gaussian, spherical, and linear models were selected for the semi-variograms. Three parameters were distinguished: the nugget variance (Co; i.e., the y-intercept of the model; the sill (Co + C; i.e., the model asymptote; and the range (A; i.e., the distance over which spatial dependence is apparent (Robertson, 2008). The nugget ratio (Co/(Co + C)) indicates the spatial dependence, i.e., a variable is considered spatially dependent if the nugget ratio is <25% (Cambardella et al., 1994).

We established regression models on the basis of our hypotheses, using crop yields and potential N_2O and CO_2 emissions as response variables and a range of soil variables as explanatory variables. Statistical analyses were carried out by R software (RCoreTeam, 2013). We used multiple linear regression models (function *lm()* in R) (James et al., 2013). Only explanatory indicators (regressors) that were sufficiently uncorrelated ($r < 0.70$) have been included in the selection process to avoid the problem of collinearity (Ott and Longnecker, 2010). In case of high correlations, one of the variables was selected for inclusion in the selection process and the other was rejected. To identify the best parameter combinations, the percentage of variance accounted for (R^2_{adj}; i.e., adjusted for the number of parameters), the value of Mallows' Cp (Ott and Longnecker, 2010), and the p value of the parameter estimates were evaluated. The selected models were based on the marginal increase of R^2_{adj} with increasing number of variables, a low Cp, and the significance of the parameters ($p < 0.05$).

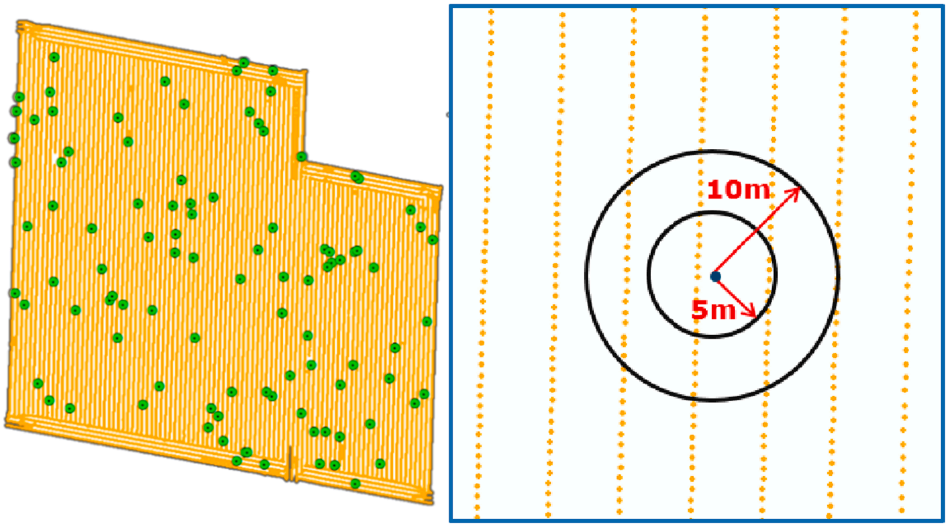

Fig. 2. Soil sampling points (green dots) in one of the fields (left panel), and a sketch of the recording of grain yield (yellow dots) with the harvester in a field (right-hand side figure). The circles indicate how grain yield recordings were allocated to a soil sampling point, in two ways, using a radius of 5 or 10 m around the soil sampling point (see text). Harvested yield recordings (yellow points) were implemented by real-time measurements and GPS equipped on the harvest machine.

3. Results and discussion

3.1. Mean soil characteristics of the four fields

Soil bulk density varied within and between fields and tended to increase with soil depth (Fig. 3). Field A had the lowest bulk density, at all three depths, and fields B and D the highest bulk density, notably in the subsoil. Field B had a mean bulk density of 1.60 ± 0.11 g cm^{-3} at 30–35 cm and field D had a mean bulk density of 1.58 ± 0.10 g cm^{-3} at 30–35 cm. The mean RND at a depth of 30–35 cm ranged from 0.86 ± 0.05 for field A to 1.03 ± 0.07 for field B, to 0.95 ± 0.06 for field C and to 1.00 ± 0.07 for field D (Tables S1, S2), indicating that mean subsoil bulk density in fields B and D is at a level where soil functioning may be impeded (van den Akker and Hoogland, 2011). This relates especially to root growth and drainage (Czyz, 2004; Alaoui et al., 2011; Matthieu et al., 2011; Berisso et al., 2012).

The increasing soil bulk density with soil depth is likely the result of both a decreasing clay content (and increasing sand content) with depth and of the use of heavy machinery (for harvesting potatoes and sugar beet, and manure application). The manure applicators and crop harvesters have become heavier over time and do contribute to the densification of the subsoil (Keller et al., 2019; Schjonning et al., 2015; van den Akker et al., 2013). A modelling study suggested that 43% of the agricultural land in the Netherlands has a compacted subsoil (Brus and Van Den Akker, 2018), but confirmation by measurements is lacking. Especially clay soils are vulnerable to compaction when wet (Horn et al., 1995).

Soil penetration resistance increased with soil depth, notably below a depth of about 30 cm (Figs. S1, S2). Spatial variations in penetration resistance readings were relatively large (c.v. ranged from 23 to 76%, Table S1). Comparisons between fields are confounded by differences in soil moisture conditions between fields due to the time differences in

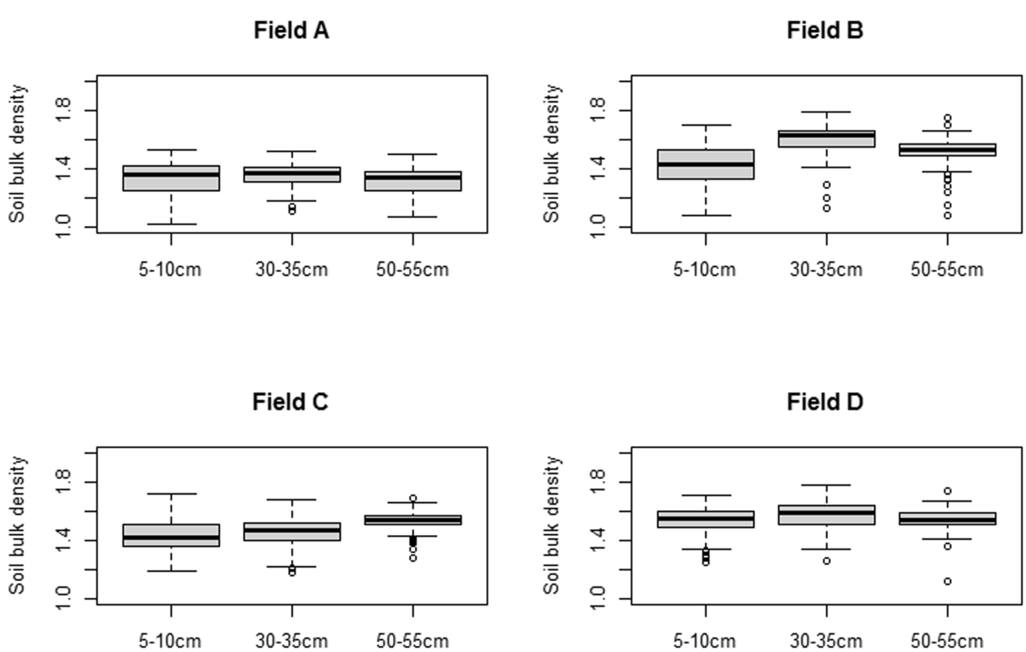

Fig. 3. Box plots of soil bulk density measurements in the four fields (A, B, C, D) at three different depths. Boxes indicate the upper (75%) and lower quartiles (25%) and the whiskers indicate the 5 and 95 percentiles. The line in the boxes indicate the median values. The unit of bulk density is g cm^{-3}.

measurements (days to weeks).

Mean soil respiration (CO_2 emissions) tended to decrease with depth in all fields. The c.v. of the mean potential CO_2 emission was about three times larger in field A than in the other fields; this is probably related to the relatively large variation in SOM content of field A (Table S1). Mean potential N_2O emissions tended to increase with depth. The ratio of potential CO_2 emissions to potential N_2O emissions also decreased with depth; this was most notable in field A (Table S1). Incidental negative N_2O emissions (apparent N_2O reduction) occurred in samples from all four fields. Coefficients of variations were larger for the potential N_2O and CO_2 emissions than for bulk density, clay and SOM contents.

Average wheat yield ranged from 7.6 ± 0.6 to 11.3 ± 0.5 Mg ha^{-1} in field A during 2015 to 2019, and from 11.0 ± 0.3 to 11.3 ± 2.4 Mg ha^{-1} in field B (Table S1). In field C, average wheat yield was 9.5 ± 0.9 and 9.7 ± 1.3 Mg ha^{-1} in 2017 and 2019, respectively. Coefficients of variations were relatively small for wheat yield in all three fields and years. There were no spatial explicit yield recordings for other crops, and no spatial explicit wheat yield data were available for field D.

3.2. Spatial variations in soil characteristics and crop yields

Within-field spatial variations were observed visually in the maps of subsoil bulk density (Fig. 4), the wheat yield maps (Fig. S3), and in the maps of potential CO_2 and N_2O emissions of the top soil (Fig. S4). These spatial patterns seemed to be related partly to the spatial patterns in soil structure of the top soil (Fig. S5) and in the clay content (not shown).

Results of semi-variogram analyses of soil variables and wheat yields of the four fields are presented in Table 1. Exponential models gave the best fit for most variables (17 out of 50 soil characteristics examined for the four fields), followed by a spherical model (15), a gaussian model (14) and a linear model (4). The correlation coefficients (R^2) of the models used were relatively high (range 0.52 to 0.97) for field A, modest (range 0.07–0.97) for field B, low to modest for field C (range 0.01–0.88) and low for field D (range 0.01–0.26). The poor fit of the models for field D may be related to the unusual narrow shape of this field, despite the fact that this field had a relatively small area (Fig. 1). We used a fixed number of 100 sampling points for all four fields, despite their different sizes and shapes, because we had no prior information about within-field spatial variations. However, this number should not be considered as the optimum number of sampling points for all fields.

The nugget effect was small in most cases (Table 1), indicating that the small-scale variance was relatively small and that the sampling design was adequate to measure the spatial variability of the studied variables (Bogunovic et al., 2017). The nugget-to-sill ratio (Co/(Co + C)) was low (<25%) for most variables, indicating that the variations in these variables were spatially dependent (Cambardella et al., 1994). Variations in soil bulk density were spatially strongly dependent at all three depths, apart from field A (at depth of 30–35 and 50–55 cm) and field B (at depth of 50–55 cm). Within-field variations in clay and SOM contents of the topsoil were also spatially strongly dependent, apart from the clay content in field D. Within-field variations in wheat yield in fields A, B and C were also spatially depended, for all years (Table 1). The same applies to the potential CO_2 and N_2O emissions during the incubation of soil samples; the within-field variations in the emissions of CO_2 and N_2O were spatially depended at all three depth, apart from three cases (two for CO_2 and one for N_2O emissions).

The range (A in Table 1) of the spatially dependent variance tended to be smaller for soil bulk density than for clay and SOM contents. It was mostly < 50 m for soil bulk density in fields B, D and C. The semi-variograms of potential CO_2 and N_2O emissions also showed a relatively small range. No attempts were made to estimate values in points at which no samples have been taken through ordinary kriging (Lipiec and Usowicz, 2018), as small ranges make spatially explicit management complicated. Wheat yields had a relatively strong spatial dependency with a range of 137 to 773 m, suggesting that some of this variation may be addressed possibly by precision management.

Within-field variations in crop yield may be caused by spatial variations in soil water and soil nutrient delivery to the crop, spatial variations in the incidence of weeds, pest and diseases, and to spatial variations in soil and crop management practices (e.g. planting density, fertilization, crop protection) (Basso et al., 2019; Maestrini and Basso, 2018; Taylor et al., 2003). Extractable nutrients (N, P, K, Mg, Cu, Zn, Se) were spatially dependent in a number of cases, with ranges varying from 12 to 1800 m (Table S3). Extractable P and K were relatively low in field B (Fig. S1), but step-wise multiple regression analyses indicated that there were no statistically significant correlations between the spatial variation of extractable P and K and spatial variations in wheat yields (not shown). We infer that it is unlikely that extractable (micro)nutrients were wheat yield limiting, although the level of some nutrients tended to be below recommended levels (Fig. S6, Table S4). We cannot exclude that spatial variations in available soil water and in the incidence of weeds and diseases have contributions to spatial variations in wheat yield. In summer, wheat roots may tap from shallow groundwater, which enters the root zone through capillary rise. This is one of the

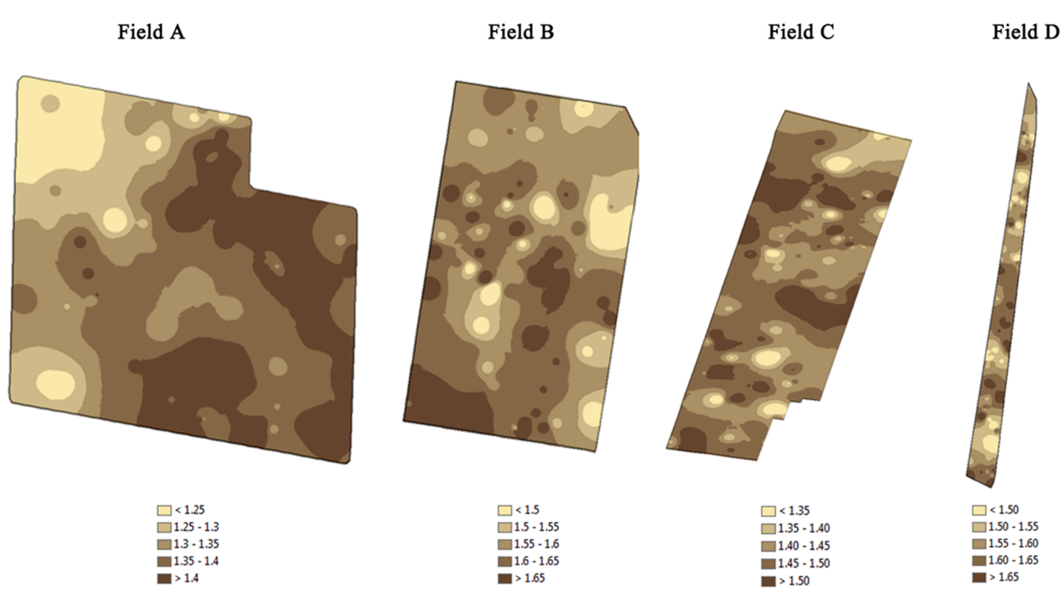

Fig. 4. Maps depicting the spatial variations of soil bulk density (g cm^{-3}) at a depth of 30–35 cm of the four fields. Note that the scaling differs between fields.

Table 1
Semi-variogram coefficients of soil properties and cereal yields of four fields. Note that emissions of CO_2 and N_2O are potential CO_2 and N_2O emissions (see text).

Fields	Variables†)	Model	Nugget, C_0 (Unit)^2	Sill, (C_0 + C) (Unit)^2	Range, A (m)	Nugget ratio, $C_0/(C_0 + C)$	R^2
A	SOM content	Gaussian	0.01	0.13	572	0.11	0.97
	Clay content	Gaussian	0.02	0.20	662	0.11	0.96
	Soil BD (0–5 cm)	Exponential	<0.01	0.01	60	<0.01	0.52
	Soil BD (30–35 cm)	Gaussian	<0.01	0.01	356	0.45	0.78
	Soil BD (50–55 cm)	Spherical	<0.01	0.01	558	0.25	0.85
	N_2O emission (5–10 cm)	Gaussian	0.13	0.64	85	0.20	0.81
	N_2O emission (30–35 cm)	Exponential	0.02	0.41	108	0.05	0.73
	N_2O emission (50–55 cm)	Spherical	0.12	0.41	187	0.28	0.83
	CO_2 emission (5–10 cm)	Exponential	<0.01	0.72	224	<0.01	0.92
	CO_2 emission (30–35 cm)	Exponential	<0.01	0.77	229	<0.01	0.93
	CO_2 emission (50–55 cm)	Spherical	0.12	0.75	175	0.15	0.86
	Wheat yield (2015)	Spherical	<0.01	0.01	418	0.21	0.85
	Wheat yield (2018)	Exponential	<0.01	0.01	576	0.19	0.91
B	SOM content	Exponential	0.01	0.05	1089	0.23	0.69
	Clay content	Gaussian	3.17	13.23	415	0.24	0.94
	Soil BD (0–5 cm)	Exponential	<0.01	0.02	13	0.07	0.07
	Soil BD (30–35 cm)	Gaussian	<0.01	0.01	22	0.03	0.50
	Soil BD (50–55 cm)	Exponential	<0.01	0.01	192	0.50	0.43
	N_2O emission (5–10 cm)	Spherical	0.01	0.13	56	0.08	0.42
	N_2O emission (30–35 cm)	Linear	0.07	0.07	241	1.00	0.08
	N_2O emission (50–55 cm)	Spherical	<0.01	0.07	22	0.05	0.32
	CO_2 emission (5–10 cm)	Exponential	0.01	0.11	37	0.11	0.43
	CO_2 emission (30–35 cm)	Spherical	0.01	0.27	36	0.02	0.42
	CO_2 emission (50–55 cm)	Exponential	0.05	0.18	177	0.30	0.90
	Wheat yield (2015)	Gaussian	<0.01	0.03	165	0.01	0.97
	Wheat yield (2019)	Exponential	<0.01	0.00	137	0.13	0.55
C	SOM content	Gaussian	<0.01	0.01	5	0.20	<0.01
	Clay content	Spherical	<0.01	0.05	24	0.08	0.05
	Soil BD (0–5 cm)	Gaussian	<0.01	0.01	24	0.18	0.43
	Soil BD (30–35 cm)	Gaussian	<0.01	0.01	19	0.17	0.05
	Soil BD (50–55 cm)	Gaussian	<0.01	<0.01	16	0.15	0.01
	N_2O emission (5–10 cm)	Exponential	0.01	0.10	29	0.15	0.07
	N_2O emission (30–35 cm)	Spherical	0.01	0.15	17	0.04	<0.01
	N_2O emission (50–55 cm)	Spherical	0.03	0.02	31	0.12	0.18
	CO_2 emission (5–10 cm)	Linear	0.06	0.06	342	1.00	0.09
	CO_2 emission (30–35 cm)	Exponential	0.01	0.09	1	0.08	<0.01
	CO_2 emission (50–55 cm)	Spherical	<0.01	0.02	21	0.04	0.03
	Wheat yield (2017)	Exponential	<0.01	0.01	268	0.12	0.88
	Wheat yield (2019)	Exponential	0.01	0.03	773	0.19	0.82
D	SOM content	Exponential	<0.01	0.02	35	0.15	0.11
	Clay content	linear	0.01	0.01	449	1.00	0.10
	Soil BD (0–5 cm)	Spherical	0.02	0.05	691	0.34	0.26
	Soil BD (30–35 cm)	Spherical	<0.01	0.01	32	0.06	0.14
	Soil BD (50–55 cm)	Gaussian	<0.01	<0.01	6	0.22	<0.01
	N_2O emission (5–10 cm)	Exponential	0.40	2.82	31	0.14	0.07
	N_2O emission (30–35 cm)	Gaussian	0.04	0.23	6	0.19	<0.01
	N_2O emission (50–55 cm)	Gaussian	0.03	0.15	20	0.19	0.01
	CO_2 emission (5–10 cm)	Spherical	0.02	0.10	72	0.20	0.18
	CO_2 emission (30–35 cm)	linear	0.07	0.07	449	1.00	0.02
	CO_2 emission (50–55 cm)	Spherical	<0.01	0.02	25	0.11	0.03

†) SOM content, g/kg; clay content, %; soil (BD) bulk density, g/cm^3; potential N_2O and CO_2 emissions, mg/m^2/d; wheat yield, Mg/ha.

reasons for the rather stable wheat yields observed during 2015–2019, next to the good management by the farmers; the relatively low yield of Field A in 2016 was related to late sowing of summer wheat.

Spatial variations in soil bulk density may also contribute to spatial variations in crop yield, notably through its effect on root growth and the delivery of soil water and nutrients. Precision agriculture aims at addressing spatial variations in soil and crop performances, and thereby may contribute to increasing yield and resource use efficiency. Precision management relies on accurate measurements and spatially distinct areas that are sufficiently large to be managed (Field et al., 2017; Diacono et al., 2013). Spatial dependencies with a (very) short range and/or low stability over years are difficult to address. Application of precision management may be limited also by the often diffuse relationships between soil characteristics and crop yields, which makes inferences about spatial variations unreliable, and by the lack of appropriate tools to communicate between precision management techniques (Kempenaar et al., 2020).

3.3. Relationships between crop yield and soil properties

Multiple linear regression analyses indicated that spatial variations in wheat yield of field A were related to spatial variations in soil clay content, bulk density, and penetration resistance at 30–35 cm in 2015 and 2016 ($P < 0.05$), but not in 2018 and 2019 (Table 2). These relationships may reflect a relationship between yield and soil water delivery to the crop (Libohova et al., 2018). Spatial variations in $CaCl_2$-extractable Mg content were related to spatial variations in wheat yield ($P < 0.001$) in Field A in 2018, but we doubt whether this is a causal relationship (Table 2). No statistically significant relationships between within-field spatial variations in wheat yield and within-field spatial variations in soil characteristics were found for field A in 2019 ($P > 0.05$, Table 2). Spatial variations in wheat yield were also significantly related to spatial variations in soil clay content in field B in 2015, but no significant relationships were found in 2016. However, spatial variations in wheat yield were not significantly related to spatial variations in soil bulk density or penetration resistance in field B, while it had a relatively

Table 2
Coefficients (means ± standard deviations) of the multiple regression relationships between wheat yield and soil characteristics of fields A, B and C. Correlations coefficients (R^2) and degree of freedom (DF) are presented at the bottom of each block.

	Field A (2015)	Field A (2016)	Field A (2018)	Field A (2019)
α (Intercept)	13.86 ± 2.16***	9.17 ± 1.47***	6.42 ± 1.75***	7.96 ± 2.4***
β_1 (Total N)	−0.54 ± 1.06	−0.8 ± 0.66	−0.43 ± 0.86	1.1 ± 1.59
β2 (SOM)	−0.35 ± 0.51	0.35 ± 0.32	0.01 ± 0.41	0.22 ± 0.66
β3 (Clay content)	0.1 ± 0.04**	0.06 ± 0.02*	0.002 ± 0.032	−0.01 ± 0.06
β4 ($CaCl_2$-extractable Mg)	0.02 ± 0.01	−0.01 ± 0.01	0.03 ± 0.01***	−0.02 ± 0.02
β5 (Bulk density in 30–35 cm)	−2.73 ± 1.36*	−0.84 ± 0.88	1.19 ± 1.1	2.19 ± 1.79
β6 (Penetration resistance in 30–35 cm)	−0.002 ± 0.001	−0.003 ± 0.001***	−0.001 ± 0.001	0.001 ± 0.001
R^2	0.23	0.48	0.23	0.16
DF	93	65	93	26
	Field B (2015)	Field B (2019)	Field C (2017)	Field C (2019)
α (Intercept)	16.94 ± 4.87***	11.28 ± 0.7***	10.3 ± 1.96***	11.87 ± 2.77***
β_1 (Total N)	−1.83 ± 4.94	−0.34 ± 0.71	−0.78 ± 1.67	−2.47 ± 2.36
β2 (SOM)	−1.28 ± 1.71	0.21 ± 0.24	0.48 ± 0.72	0.83 ± 1.02
β3 (Clay content)	0.31 ± 0.15*	0.01 ± 0.02	−0.02 ± 0.04	0.01 ± 0.06
β4 ($CaCl_2$-extractable Mg)	−0.01 ± 0.03	−0.002 ± 0.004	0.01 ± 0.01	0.01 ± 0.02
β5 (Bulk density in 30–35 cm)	−0.71 ± 2.36	−0.25 ± 0.34	−0.95 ± 0.98	−1.14 ± 1.39
β6 (Penetration resistance in 30–35 cm)	−0.001 ± 0.003	−0.0005 ± 0.0004	−0.0002 ± 0.0014	0.001 ± 0.002
R^2	0.18	0.06	0.03	0.02
DF	92	92	93	93

†) Multiple linear regression models (function *lm()* in R, James et al., 2013). The same as below.
††) Total N and SOM contents, g/kg; clay content, %; available Mg, mg/kg; soil (BD) bulk density, g/cm^3; penetration resistance, kPa. The same as below.
†††) "*" means $0.01 < P < 0.05$, "**" means $0.001 < P < 0.01$, "***" means $P < 0.001$. The same as below.

high subsoil bulk density and a Relative Normalized Density above 1 (Tables 2 and S2). Further, spatial variations in crop yield in field C were not significantly related to spatial variations in soil properties (Table 2). Evidently, the relationships between spatial variations in crop yield and soil characteristics were not stable over years, likely because of interactions as a result of differences between years in weather conditions. As a consequence, it will be difficult to address the spatial variations adequately through precision agriculture technology.

Few studies have related spatial variations in subsoil bulk density to spatial variations in crop yield, mainly because subsoil bulk density and spatial variations in subsoil bulk density cannot be measured easily (Keller et al., 2017; Horn et al., 1995). Bölenius et al., (2018) found significant relationships between spatial variations in penetration resistance and spatial variations in crop yields, but these were strongly dependent on season and weather conditions. They concluded that single measurements of penetration resistance were insufficient to identify yield variations, apart from dry years. Usowicz and Lipiec (2017) found statistically significant negative relationships between spatial variations in cereal yields and spatial variations in top soil (0–10 cm) bulk density of a 1 ha large experimental field. The spatial dependence was strong and the range varied from 12 to 99 m between years (repeated measurements in the same field). However, subsoil compaction (or bulk density) was not measured. Lipiec and Usowicz (2018) found no statistically significant relationships between spatial variations in cereal yields and spatial variations in top soil (0–10 cm) bulk density of a 2.4 ha large farmers' field. Again, subsoil bulk density was not measured. Further, spatial variations in topsoil (0–20 cm) bulk density were negatively related to spatial variations in saturated hydraulic conductivity of soils at regional scale (140 km^2), while variations in bulk density were relatively small and only weakly spatial dependent (Usowicz and Lipiec, 2021). These studies clearly indicate that soil bulk density may be an important crop-yield influencing factor, but that data and information about the relationships between variations in subsoil bulk density and crop yield are often confounded by soil water contents.

3.4. Relationships between soil bulk density and potential CO_2 and N_2O emissions

Soil CO_2 respiration reflects soil biological activity (Avidano et al., 2005); it is primarily related to the amounts of metabolizable organic matter, temperature and soil aeration. Soil N_2O emission reflects the balance between N_2O production and consumption by micro-organisms in soil, and is related to the concentrations of ammonium (NH_4^+), nitrate (NO_3^-) and metabolizable organic matter, as well as to temperature and soil aeration (Wrage-Monnig et al., 2018; Kool et al., 2010; Bange, 2000). We hypothesized that spatial variations in potential CO_2 and N_2O emissions were related to spatial variations in soil bulk density, as soil bulk density affects soil aeration. Indeed, within-field variations in potential CO_2 emissions were often significantly related to within-field variations in soil bulk density in the subsoil at 30–35 cm in all four fields, and in two fields also at depth of 50–55 cm (Table 3). Also, variations in potential N_2O emissions were significantly related to variations in soil bulk density of the top soil in fields A and B and to variations in bulk density in the subsoil at depth of 30–35 cm in field A, and 50–55 cm of fields A and D (Table 3). Spatial variations in potential CO_2 and N_2O emissions were not related to spatial variations in the SOM content of the topsoil in any of the four fields.

Commonly, an increase in soil bulk density decreases CO_2 emissions and increases N_2O emissions (Bessou et al., 2010; Ruser et al., 2006; van Groenigen et al., 2005; Sitaula et al., 2000). Increases in soil bulk density decrease soil porosity and aeration, and thereby decrease soil respiration but increase N_2O production (or reduce N_2O diffusion and N_2O consumption rates). Changes in the ratio of soil CO_2 and N_2O emissions in response to changes in soil bulk density may thus provide insight into differential perturbations of soil C and N transformations. Frequency distributions of potential CO_2 and N_2O emissions were highly skewed in all fields, and therefore logarithmic values were used. The ratio of log CO_2 emissions to log N_2O emissions tended to decrease with an increase in soil bulk density, especially in field B (Fig. 5), the field with the highest mean bulk density and also with the highest coefficient of variation of the mean bulk density (Table S1). This indicates that potential N_2O emissions increased relative to potential CO_2 emissions with increasing bulk density. Further, the ratio of log CO_2 emissions to log N_2O emissions strongly decreased with bulk density following N application (Fig. 5). Emissions of N_2O in the top soil (5–10 cm) and sub soil (30–35 cm) increased by a factor of 2 to 5 following addition of $NaNO_3$, suggesting that the N_2O emissions were in part nitrate limited. Evidently, increases in N_2O emissions following N fertilization were much greater in soil with high bulk density than in soil with low bulk density. Note that the increased N_2O emissions in the top soil (0–5 cm) vanished after 6 days and that the peak in the subsoil at 30–35 cm occurred much later than in the top soil. No increases in N_2O emissions occurred following N application to the subsoil at 50–55 cm during the six-days measuring period (Fig. 5).

Our results provide further evidence that the current trend of increasing wheel loads in modern agriculture, which increase (sub)soil bulk density, may increase N_2O emissions from soil and especially also from the subsoil (Shcherbak and Robertson, 2019). Agriculture is a main

Table 3

Coefficients (means ± standard deviations) of the multiple regression relationships between potential N_2O emissions, potential CO_2 emissions and soil characteristics at depth of 5–10, 30–35, and 50–55 cm of the four fields. Correlations coefficients (R^2) and degree of freedom (DF) are presented at the bottom of each block.

	Field A	Field B	Field C	Field D
N_2O emission (5–10 cm)				
α (Intercept)	−3.21 ± 1.29*	−0.28 ± 0.26	1.36 ± 0.49**	1.63 ± 2.29
β_1 (Clay content)	0.02 ± 0.03	0.01 ± 0.01	0.03 ± 0.01***	0.03 ± 0.08
β2 (SOM)	−0.61 ± 0.4	0.1 ± 0.11	0.2 ± 0.2	−2.34 ± 1.3
β3 (Bulk density at 5–10 cm)	3.38 ± 0.82***	0.42 ± 0.13**	−0.23 ± 0.26	0.22 ± 0.9
β4 (Penetration resistance 5–10 cm)	−0.001 ± 0.002	−0.0003 ± 0.0007	0.0004 ± 0.0006	−0.001 ± 0.005
β5 (Total N)	1.05 ± 0.85	0.1 ± 0.33	−0.83 ± 0.45	3.87 ± 2.78
R^2	0.25	0.21	0.15	0.08
DF	86	88	87	71
CO_2 emission (5–10 cm)				
α (Intercept)	−17.41 ± 10.34	−0.18 ± 1.42	7.09 ± 1.45***	7.17 ± 2.16**
β_1 (Clay content)	−0.39 ± 0.25	−0.02 ± 0.05	−0.03 ± 0.02	−0.02 ± 0.06
β2 (SOM)	−5.01 ± 3.26	−0.6 ± 0.69	0.28 ± 0.56	−1.42 ± 0.75
β3 (Bulk density at 5–10 cm)	19.5 ± 6.58**	1.07 ± 0.72	−1.36 ± 0.79	−2.42 ± 1.11*
β4 (Penetration resistance 5–10 cm)	0.01 ± 0.01	0.002 ± 0.004	0.0001 ± 0.0016	0.001 ± 0.004
β5 (Total N)	12.44 ± 6.95	2.74 ± 1.92	−0.08 ± 1.32	3.65 ± 1.78*
R^2	0.23	0.07	0.07	0.09
DF	87	90	87	91
N_2O emission (30–35 cm)				
α (Intercept)	−3.46 ± 1.32*	1.15 ± 0.37**	0.88 ± 0.62	1.99 ± 0.82*
β1 (Bulk density at 30–35 cm)	3.48 ± 0.98***	−0.04 ± 0.23	0.34 ± 0.42	−0.35 ± 0.52
β2 (Penetration resistance 30–35 cm)	0.002 ± 0.001	−0.0005 ± 0.0003	−0.0003 ± 0.0006	−0.002 ± 0.001
R^2	0.17	0.04	0.01	0.04
DF	89	93	94	93
CO_2 emission (30–35 cm)				
α (Intercept)	−25.13 ± 8.39**	5.43 ± 1.08***	19.34 ± 1.84***	9.07 ± 1.2***
β1 (Bulk density at 30–35 cm)	22.31 ± 6.15***	−2.23 ± 0.67**	−9.5 ± 1.25***	−2.95 ± 0.76***
β2 (Penetration resistance 30–35 cm)	0.008 ± 0.007	0.0007 ± 0.0007	−0.0018 ± 0.0016	−0.002 ± 0.001
R^2	0.14	0.12	0.39	0.16
DF	95	94	93	91
N_2O emission (50–55 cm)				
α (Intercept)	−5.11 ± 2.28*	2.08 ± 0.58***	3.26 ± 1.28*	4.62 ± 1.23***
β1 (Bulk density at 50–55 cm)	6.02 ± 1.81**	−0.47 ± 0.39	−0.84 ± 0.8	−2.08 ± 0.79**
β2 (Penetration resistance 50–55 cm)	−0.001 ± 0.001	0.00005 ± 0.00032	−0.0014 ± 0.001	0.0002 ± 0.0006
R^2	0.11	0.01	0.03	0.07
DF	95	95	92	96
CO_2 emission (50–55 cm)				
α (Intercept)	−9.39 ± 7.23	5.18 ± 0.95***	5.2 ± 1.41***	5.2 ± 1.41***
β1 (Bulk density at 50–55 cm)	12.73 ± 5.72*	−2.18 ± 0.64***	−0.49 ± 0.88	−0.49 ± 0.88
β2 (Penetration resistance 50–55 cm)	−0.003 ± 0.004	0.0001 ± 0.0005	0.00004 ± 0.00106	0.00004 ± 0.00106
R^2	0.05	0.12	0.01	0.01
DF	94	91	94	94

source of greenhouse emissions and N_2O emissions form a significant fraction of the total GHG emissions from agriculture. Spatial variations in soil bulk density are likely also an important explanatory factor for the large spatial variations in N_2O emissions observed in the current study (Table S1) and in other studies (Robertson and Groffman, 2015).

4. Conclusions

Our initial hypotheses were only partly proven. We found significant variations in subsoil bulk density, which were spatially dependent, but the level of soil compaction appeared to be nowhere severe in the four fields. Further, within-field spatial variations in subsoil bulk density were related to within-field spatial variations in the potential emissions of CO_2 and N_2O, but not to variations in wheat yield.

Our random sampling approach yielded unbiased estimates of the spatial variations in subsoil bulk density and other soil properties within four fields, which were greatly different in shape and size. Most of these variations were strongly spatially dependent but the ranges were often relatively small, indicating that the scope for identifying distinctly different and manageable units was relatively small. Yet, semi-variograms proved to be an effective method to characterize spatial variations in both soil properties, soil processes and crop yields.

The mean bulk density of the subsoil in two fields was close to the suggested threshold of where bulk density affects soil functioning. Indeed, potential emissions of CO_2 and N_2O were significantly related to soil bulk density. The ratio of CO_2 emissions to N_2O emissions was negatively related to bulk density in both topsoil and subsoil, especially following N application, indicating that emissions of N_2O increased with an increase in soil bulk density. More studies are needed to find out how stable these relationships are over years, and how precision agriculture may address these relationships.

Spatial variations in wheat yield were only marginally related to soil properties. No statistically significant relationships were found between within-field spatial variations in (sub)soil bulk density and within-field spatial variations in wheat yield in any of the 8 field × year combinations analyzed. Variations in wheat yield were spatially dependent, and the ranges were on average larger than the ranges of soil properties, suggesting that spatial variations in wheat yield were mainly caused by other (management) factors. The near absence of a relationship between within-field variations in soil properties and within-field variations in wheat yield is likely also related to the fact that the within-field variations in soil properties were relatively small, that wheat is not a very sensitive crop to subsoil compaction, and that crop growth conditions are relatively good in the study area.

The farmers were not surprised by the findings of relatively high soil bulk density values in some fields, which they ascribed to effects of heavy harvesters and manure applicators. Increasingly, they use GPS-controlled trafficking to minimize the area and extent of soil compaction, as they are aware that there are as yet no easy-to-implement remediation measures for spatial variations in subsoil compaction.

Our study provides evidence that potential N_2O emissions (and the ratio of potential CO_2 emissions to potential N_2O emissions) is a more sensitive indicator for the effect of soil bulk density on soil functioning than wheat yield. The linear relationship between bulk density and the

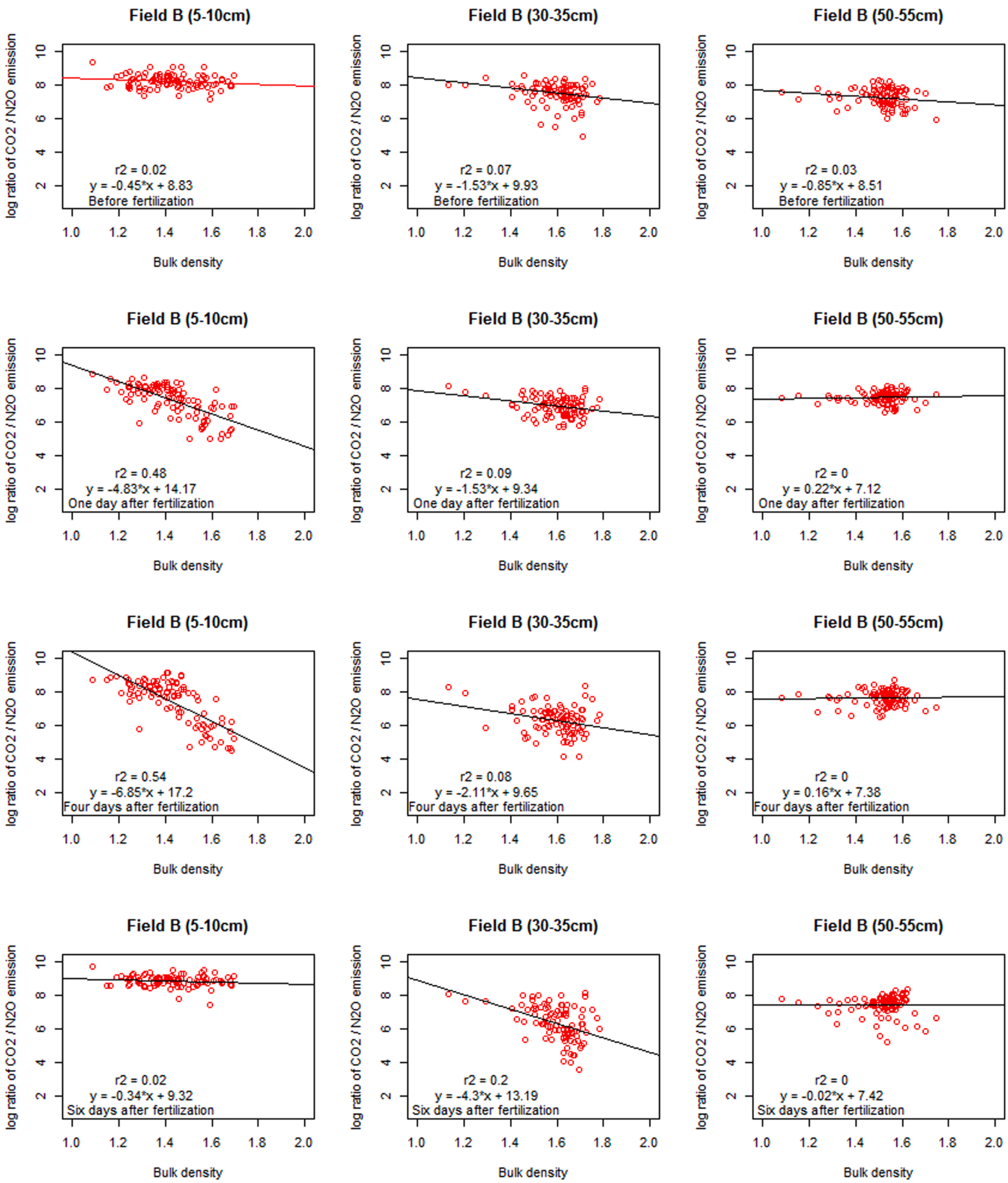

Fig. 5. Relationships between soil bulk density (g cm^{-3}) and the ratio of potential CO_2 emissions and potential N_2O emissions (mg m^{-2} d^{-1}; log scale) for field B at three different depth intervals and at four different moments in time.

ratio of CO_2 emissions to N_2O emissions was apparent in both top soil (5–10 cm) and subsoil (30–35 cm). This linear relationship also suggests that there was no specific threshold for soil bulk density beyond which emissions change dramatically; instead emissions change gradually with an increase in bulk density.

Our results provide also evidence that an increasing soil compaction in modern agriculture contributes to increases in N_2O emissions from agricultural land and that these increases in emissions may emerge from the top soil as well as the subsoil. Future studies should consider N_2O emission factors as function of N fertilizers and (sub)soil bulk density.

Declaration of Competing Interest

The authors declare that they have no known competing financial interests or personal relationships that could have appeared to influence the work reported in this paper.

Acknowledgements

This project has received funding from the European Union's Horizon 2020 research and innovation programme under grant agreement No 677407 (SoilCare project), and from China Scholarship Council (File No. 201408130093). We gratefully acknowledge the support from the farmers in the project H-Wodka, and from Eurofins-Agro.

Appendix A. Supplementary data

Supplementary data to this article can be found online at https://doi.org/10.1016/j.catena.2022.106156.

References

Alaoui, A., Lipiec, J., Gerke, H.H., 2011. A review of the changes in the soil pore system due to soil deformation: A hydrodynamic perspective. Soil Tillage Res. 115, 1–15. https://doi.org/10.1016/j.still.2011.06.002.

ASABE (2006) Procedures for using and reporting data obtained with the soil cone penetrometer. EP542 FEB99, St. Joseph, Michigan, 1052-1055. American Society of Agricultural and Biological Engineers.

Avidano, L., Gamalero, E., Cossa, G.P., Carraro, E., 2005. Characterization of soil health in an Italian polluted site by using microorganisms as bioindicators. Appl. Soil Ecol. 30 (1), 21–33. https://doi.org/10.1016/j.apsoil.2005.01.003.

Awal, R., Safeeq, M., Abbas, F., Fares, S., Deb, S.K., Ahmad, A., Fares, A., 2019. Soil physical properties spatial variability under long-term no-tillage corn. Agronomy 9 (11), 750. https://doi.org/10.3390/agronomy9110750.

Banerjee, S., Walder, F., Büchi, L., Meyer, M., Held, A.Y., Gattinger, A., Keller, T., Charles, R., Van Der Heijden, M.G., 2019. Agricultural intensification reduces microbial network complexity and the abundance of keystone taxa in roots. The ISME J. 13 (7), 1722–1736. https://doi.org/10.1038/s41396-019-0383-2.

Bange, H.W., 2000. Global change - It's not a gas. Nature 408 (6810), 301–302. https://doi.org/10.1038/35042656.

Barik, K., Aksakal, E.L., Islam, K.R., Sari, S., Angin, I., 2014. Spatial variability in soil compaction properties associated with field traffic operations. Catena 120, 122–133. https://doi.org/10.1016/j.catena.2014.04.013.

Basso, B., Shuai, G., Zhang, J., Robertson, G.P., 2019. Yield stability analysis reveals sources of large-scale nitrogen loss from the US Midwest. Sci. Rep.-Uk 9 (1). https://doi.org/10.1038/s41598-019-42271-1.

Berisso, F.E., Schjonning, P., Keller, T., Lamande, M., Etana, A., de Jonge, L.W., Iversen, B.V., Arvidsson, J., Forkman, J., 2012. Persistent effects of subsoil compaction on pore size distribution and gas transport in a loamy soil. Soil Tillage Res. 122, 42–51. https://doi.org/10.1016/j.still.2012.02.005.

Bessou, C., Mary, B., Leonard, J., Roussel, M., Grehan, E., Gabrielle, B., 2010. Modelling soil compaction impacts on nitrous oxide emissions in arable fields. Eur. J. Soil Sci. 61 (3), 348–363. https://doi.org/10.1111/j.1365-2389.2010.01243.x.

Bogunovic, I., Trevisani, S., Seput, M., Juzbasic, D., Durdevic, B., 2017. Short-range and regional spatial variability of soil chemical properties in an agro-ecosystem in eastern Croatia. Catena 154:50-62. doi:j.catena.2017.02.018.

Bölenius, E., Wetterlind, J., Keller, T., 2018. Can within field yield variation be explained using horizontal penetrometer resistance and electrical conductivity measurements? Results from three Swedish fields. Acta Agriculturae Scandinavica, Section B—Soil & Plant Science 68 (8), 690–700. https://doi.org/10.1080/09064710.2018.1464201.

Brus, D.J., Van Den Akker, J.J., 2018. How serious a problem is subsoil compaction in the Netherlands? A survey based on probability sampling. Soil 4 (1), 37–45. https://doi.org/10.5194/soil-4-37-2018.

Cambardella, C.A., Moorman, T.B., Novak, J., Parkin, T., Karlen, D., Turco, R., Konopka, A., 1994. Field-scale variability of soil properties in central Iowa soils. Soil Sci. Soc. Am. J. 58 (5), 1501–1511. https://doi.org/10.2136/sssaj1994.03615995005800050033x.

Chamen, W.C.T., Moxey, A.P., Towers, W., Balana, B., Hallett, P.D., 2015. Mitigating arable soil compaction: A review and analysis of available cost and benefit data. Soil Tillage Res. 146, 10–25. https://doi.org/10.1016/j.still.2014.09.011.

Crittenden, S.J., Huerta, E., de Goede, R.G.M., Pulleman, M.M., 2015. Earthworm assemblages as affected by field margin strips and tillage intensity: An on-farm approach. Eur. J. Soil Biol. 66, 49–56. https://doi.org/10.1016/j.ejsobi.2014.11.007.

Czyz, E.A., 2004. Effects of traffic on soil aeration, bulk density and growth of spring barley. Soil Tillage Res. 79 (2), 153–166. https://doi.org/10.1016/j.still.2004.07.004.

Diacono, M., Rubino, P., Montemurro, F., 2013. Precision nitrogen management of wheat. A review. Agronomy for Sustainable Development 33 (1), 219–241. https://doi.org/10.1007/s13593-012-0111-z.

Ecorys, 2007. Green- blue veining: agrobiodiversity as innovation for sustainable agriculture. ECORYS Nederland BV, Rotterdam. 27 pp.

Field, C.R., Dayer, A.A., Elphick, C.S., 2017. Landowner behavior can determine the success of conservation strategies for ecosystem migration under sea-level rise. P. Natl. Acad. Sci. U.S.A. 114 (34), 9134–9139. https://doi.org/10.1073/pnas.1620319114.

Hamza, M.A., Anderson, W.K., 2005. Soil compaction in cropping systems - A review of the nature, causes and possible solutions. Soil Tillage Res. 82 (2), 121–145. https://doi.org/10.1016/j.still.2004.08.009.

Hohn, M., 1998. Geostatistics and petroleum geology. Springer Science & Business Media.

Horn, R., Domżżał, H., Słowińska-Jurkiewicz, A., Van Ouwerkerk, C., 1995. Soil compaction processes and their effects on the structure of arable soils and the environment. Soil Tillage Res. 35 (1–2), 23–36. https://doi.org/10.1016/0167-1987(95)00479-C.

Huber, S., Prokop, G., Arrouays, D., Banko, G., Bispo, A., Jones, R., Kibblewhite, M., Lexer, W., Möller, A., Rickson, R., 2008. Environmental assessment of soil for monitoring: volume I, indicators & criteria. Office for the Official Publications of the European Communities, Luxembourg.

James, G., Witten, D., Hastie, T., Tibshirani, R., 2013. An introduction to statistical learning,, vol 112. Springer.

Kassambara, A., 2019. Practical Statistics in R II-Comparing Groups: Numerical Variables. Datanovia.

Keller, T., Colombi, T., Ruiz, S., Manalili, M.P., Rek, J., Stadelmann, V., Wunderli, H., Breitenstein, D., Reiser, R., Oberholzer, H., Schymanski, S., Romero-Ruiz, A., Linde, N., Weisskopf, P., Walter, A., Or, D., 2017. Long-term soil structure observatory for monitoring post-compaction evolution of soil structure. Vadose Zone J. 16 (4) https://doi.org/10.2136/vzj2016.11.0118.

Keller, T., Lamand, M., Peth, S., Berli, M., Delenne, J.-Y., Baumgarten, W., Rabbel, W., Radja, F., Rajchenbach, J., Selvadurai, A.P.S., Or, D., 2013. An interdisciplinary approach towards improved understanding of soil deformation during compaction. Soil Tillage Res. 128, 61–80. https://doi.org/10.1016/j.still.2012.10.004.

Keller, T., Sandin, M., Colombi, T., Horn, R., Or, D., 2019. Historical increase in agricultural machinery weights enhanced soil stress levels and adversely affected soil functioning. Soil Tillage Res. 194, 104293. https://doi.org/10.1016/j.still.2019.104293.

Kempenaar, C., Mollema, R., Been, T., Boheemen, K.v., Biewenga, G., Burg, S.v.d., Wassenaer, L.v., Meij, K.v.d., Graumans, C., Horst, A.t., Janssen, S., Lokhorst, K., Sijbrandij, F., Steinbusch, M., Vlugt, P.v.d., Wal, T.v.d., 2020. Bottlenecks in precision agriculture at farm level - data management and exchange (in Dutch). Report WPR-10.18174/532701. Wageningen Research. doi:10.18174/532701.

Kerry, R., Oliver, M., 2007. Comparing sampling needs for variograms of soil properties computed by the method of moments and residual maximum likelihood. Geoderma. 140. 10.1016/j.geoderma.2007.04.019.

Kool, D.M., Wrage, N., Zechmeister-Boltenstern, S., Pfeffer, M., Brus, D., Oenema, O., Van Groenigen, J.W., 2010. Nitrifier denitrification can be a source of N2O from soil: a revised approach to the dual-isotope labelling method. Eur. J. Soil Sci. 61 (5), 759–772. https://doi.org/10.1111/j.1365-2389.2010.01270.x.

Lawrence, P.G., Roper, W., Morris, T.F., Guillard, K., 2020. Guiding soil sampling strategies using classical and spatial statistics: A review. Agron. J. 112 (1), 493–510. https://doi.org/10.1002/agj2.20048.

Libohova, Z., Seybold, C., Wysocki, D., Wills, S., Schoeneberger, P., Williams, C., Lindbo, D., Stott, D., Owens, P.R., 2018. Reevaluating the effects of soil organic matter and other properties on available water-holding capacity using the National Cooperative Soil Survey Characterization Database. J. Soil Water Conserv. 73 (4), 411–421. https://doi.org/10.2489/jswc.73.4.411.

Lipiec, J., Usowicz, B., 2018. Spatial relationships among cereal yields and selected soil physical and chemical properties. Sci. Total Environ. 633, 1579–1590. https://doi.org/10.1016/j.scitotenv.2018.03.277.

Lloyd, C.D., 2005. Assessing the effect of integrating elevation data into the estimation of monthly precipitation in Great Britain. J. Hydrol. 308 (1–4), 128–150. https://doi.org/10.1016/j.jhydrol.2004.10.026.

Maestrini, B., Basso, B., 2018. Drivers of within-field spatial and temporal variability of crop yield across the US Midwest. Sci. Rep.-Uk 8 (1). https://doi.org/10.1038/s41598-018-32779-3.

Matthieu, D.E., Bowman, D.C., Thapa, B.B., Cassel, D.K., Rufty, T.W., 2011. Turfgrass root response to subsurface soil compaction. Commun. Soil Sci. Plant Anal. 42 (22), 2813–2823. https://doi.org/10.1080/00103624.2011.622826.

Mueller, L., Kay, B.D., Hu, C.S., Li, Y., Schindler, U., Behrendt, A., Shepherd, T.G., Ball, B. C., 2009. Visual assessment of soil structure: Evaluation of methodologies on sites in Canada, China and Germany Part I: Comparing visual methods and linking them with soil physical data and grain yield of cereals. Soil Tillage Res. 103 (1), 178–187. https://doi.org/10.1016/j.still.2008.12.015.

Ott, R.L., Longnecker, M., 2010. An introduction to statistical methods and data analysis. 6th edition. *Cengage*, Florence, Italy.

Pulido Moncada, M., Gabriels, D., Lobo, D., Rey, J.C., Cornelis, W.M., 2014. Visual field assessment of soil structural quality in tropical soils. Soil Tillage Res. 139, 8–18. https://doi.org/10.1016/j.still.2014.01.002.

RCoreTeam, 2013. R: A Language and Environment for Statistical Computing. R Foundation for Statistical Computing, Vienna.

Robertson, G., 2008. GS+:"Geostatistics for the Environmental Sciences", Gamma Design Software, Plainwell, Michigan USA. Pdf document available for free at: https://geostatistics com/files/GSPlusUserGuide pdf.

Robertson, G.P., Groffman, P.M., 2015. Nitrogen transformations. Soil microbiology, ecology and biochemistry. Academic Press, Massachusetts, USA.

Ruser, R., Flessa, H., Russow, R., Schmidt, G., Buegger, F., Munch, J.C., 2006/ Emission of N2O, N-2 and CO2 from soil fertilized with nitrate: Effect of compaction, soil moisture and rewetting. Soil Biology & Biochemistry 38 (2):263–274. https://doi.org/10.1016/j.soilbio.2005.05.005.

Schjonning, P., van den Akker, J.J.H., Keller, T., Greve, M.H., Lamande, M., Simojoki, A., Stettler, M., Arvidsson, J., Breuning-Madsen, H., 2015. Driver-Pressure-State-Impact-Response (DPSIR) Analysis and Risk Assessment for Soil Compaction-A European Perspective. Adv. Agron. 133:183-237. doi:10.1016/bs.agron.2015.06.001.

Reijneveld, J.A., Van Oostrum, M.J., Brolsma, K.M., Fletcher, D., Oenema, O., 2022. Empower innovations in routine soil testing. Agronomy 12, 191. https://doi.org/10.3390/agronomy12010191.

Shah, A.N., Tanveer, M., Shahzad, B., Yang, G.Z., Fahad, S., Ali, S., Bukhari, M.A., Tung, S.A., Hafeez, A., Souliyanonh, B., 2017. Soil compaction effects on soil health and crop productivity: an overview. Environ. Sci. Pollut. R 24 (11), 10056–10067. https://doi.org/10.1007/s11356-017-8421-y.

Shcherbak, I., Robertson, G.P., 2019. Nitrous oxide (N2O) emissions from subsurface soils of agricultural ecosystems. Ecosystems 22 (7), 1650–1663. https://doi.org/10.1007/s10021-019-00363-z.

Sitaula, B.K., Hansen, S., Sitaula, J.I.B., Bakken, L.R., 2000. Methane oxidation potentials and fluxes in agricultural soil: Effects of fertilisation and soil compaction. Biogeochemistry 48 (3), 323–339. https://doi.org/10.1023/A:1006262404600.

Steingrover, E.G., Geertsema, W., van Wingerden, W.K.R.E., 2010. Designing agricultural landscapes for natural pest control: a transdisciplinary approach in the Hoeksche Waard (The Netherlands). Landscape Ecol. 25 (6):825-838. doi:10.1007/s10980-010-9489-7.

Stolte, J., Tesfai, M., Øygarden, L., Kværnø, S., Keizer, J., Verheijen, F., Panagos, P., Ballabio, C., Hessel, R., 2015. Soil threats in Europe. Publications Office Luxembourg.

Taylor, J.C., Wood, G.A., Earl, R., Godwin, R.J., 2003. Soil factors and their influence on within-field crop variability, part II: Spatial analysis and determination of management zones. Biosyst. Eng. 84 (4), 441–453. https://doi.org/10.1016/S1537-5110(03)00005-9.

Usowicz, B., Lipiec, J., 2017. Spatial variability of soil properties and cereal yield in a cultivated field on sandy soil. Soil Tillage Res. 174, 241–250. https://doi.org/10.1016/j.still.2017.07.015.

Usowicz, B., Lipiec, J., 2021. Spatial variability of saturated hydraulic conductivity and its links with other soil properties at the regional scale. Sci. Rep.-Uk 11 (1), 1–12. https://doi.org/10.1038/s41598-021-86862-3.

van den Akker, J., de Vries, F., Vermeulen, G., Hack-ten Broeke, M., Schouten, T., 2013. Risico op ondergrondverdichting in het landelijk gebied kaart. Alterra, Wageningen-UR.

van den Akker, J.J.H., Hoogland, T., 2011. Comparison of risk assessment methods to determine the subsoil compaction risk of agricultural soils in The Netherlands. Soil Tillage Res. 114 (2), 146–154. https://doi.org/10.1016/j.still.2011.04.002.

van Erp, P.J., Houba, V.J.G., Van Beusichem, M.L., 1998. One hundredth molar calcium chloride extraction procedure. Part I: A review of soil chemical, analytical, and plant nutritional aspects. Communications in Soil Science and Plant Analysis 29 (11-14): 1603-1623. doi:Doi 10.1080/00103629809370053.

van Groenigen, J.W., Kuikman, P.J., de Groot, W.J.M., Velthof, G.L., 2005. Nitrous oxide emission from urine-treated soil as influenced by urine composition and soil physical conditions. Soil Biol. Biochem. 37 (3), 463–473. https://doi.org/10.1016/j.soilbio.2004.08.009.

Wahlström, E.M., Kristensen, H.L., Thomsen, I.K., Labouriau, R., Pulido-Moncada, M., Nielsen, J.A., Munkholm, L.J., 2021. Subsoil compaction effect on spatio-temporal root growth, reuse of biopores and crop yield of spring barley. Eur. J. Agron. 123, 126225. https://doi.org/10.1016/j.eja.2020.126225.

Wrage-Monnig, N., Horn, M.A., Well, R., Muller, C., Velthof, G., Oenema, O., 2018. The role of nitrifier denitrification in the production of nitrous oxide revisited. Soil Biology & Biochemistry 123:A3-A16. doi:10.1016/j.soilbio.2018.03.020.

WRB F, 2006. World reference base for soil resources 2006: A framework for international classification, correlation and communication. FAO, Rome.